

## **$\Lambda^*$ matter and its stability**

J. Hrtáková<sup>a,\*</sup>, M. Schäfer<sup>a,b</sup>, and J. Mareš<sup>a</sup>

<sup>a</sup> Nuclear Physics Institute CAS, 250 68 Rez, Czech Republic

\*E-mail: hrtankova@ujf.cas.cz

<sup>b</sup> Faculty of Nuclear Sciences and Physical Engineering, Czech Technical University in Prague, 115 19 Prague 1, Czech Republic

A. Gal, E. Friedman, and N. Barnea

Racah Institute of Physics, The Hebrew University, 91904 Jerusalem, Israel

We performed calculations of nuclear systems composed solely of  $\Lambda^*$  hyperons, aiming at exploring the possibility of existence of absolutely stable  $\Lambda^*$  matter. We considered  $\Lambda^*$  interaction strengths compatible with the  $\Lambda^*\Lambda^*$  binding energy  $B_{\Lambda^*\Lambda^*}$  given by the  $\bar{K}N$  interaction model by Yamazaki and Akaishi<sup>1</sup>. We found that the binding energy per  $\Lambda^*$  saturates at values well below 100 MeV for mass number  $A \geq 120$ . The  $\Lambda^*$  matter is thus highly unstable against strong interaction decay.

*Keywords:* Strange matter;  $\Lambda^*$  resonance; SVM; RMF.

### **1. Introduction**

This contribution concerns our recent study of  $\Lambda^*$  nuclei<sup>2</sup>, which was stirred up by a conjecture about absolutely stable charge-neutral baryonic matter composed solely of  $\Lambda(1405)$  ( $\Lambda^*$ ) hyperons<sup>3</sup>.

We calculated  $\Lambda^*$  few-body systems within the Stochastic Variational Method (SVM)<sup>4</sup>, as well as  $\Lambda^*$  many-body systems within the Relativistic Mean Field (RMF) approach<sup>5</sup>. The meson-exchange  $\Lambda^*$  potentials applied in our work were fitted to reproduce the  $\Lambda^*\Lambda^*$  binding energy  $B_{\Lambda^*\Lambda^*} = 40$  MeV, given by the phenomenological  $\bar{K}N$  interaction model<sup>1</sup>. We recall that the  $\bar{K}N$  potentials used by Akaishi and Yamazaki<sup>1,3</sup>, fitted for  $I = 0$  to the mass and width of the  $\Lambda(1405)$  resonance, fail to reproduce  $K^-$  single-nucleon absorption fractions deduced from  $K^-$  capture bubble chamber experiments<sup>6</sup>. Nevertheless, we employed these very strong potentials in order to demonstrate that while solving the  $A$ -body Schrödinger equation for purely attractive  $\Lambda^*\Lambda^*$  interactions will inevitable lead to collapse, with the binding energy per particle diverging as  $A$  increases, this

scenario promoted in ref.<sup>3</sup> is unlikely in standard many-body approaches. In the following sections, we discuss only briefly our main results; more details can be found in ref.<sup>2</sup>.

## 2. $\Lambda^*$ Few-Body Systems

We started our study of  $\Lambda^*$  nuclei by calculations of few-body systems within the Stochastic Variational Method<sup>4</sup> for the meson-exchange potentials of the Dover-Gal form<sup>7</sup>:

$$V_{\Lambda^*\Lambda^*}(r) = g_{\omega\Lambda^*}^2 \left(1 - \frac{1}{8} \frac{m_\omega^2}{M_{\Lambda^*}^2}\right) Y_\omega(r) - g_{\sigma\Lambda^*}^2 \left(1 - \frac{1}{8} \frac{m_\sigma^2}{M_{\Lambda^*}^2}\right) Y_\sigma(r) + g_{\omega\Lambda^*}^2 \frac{1}{6} \left(\frac{m_\omega}{M_{\Lambda^*}}\right) Y_\omega(r) (\vec{\sigma}_1 \cdot \vec{\sigma}_2), \quad (1)$$

or the Machleidt form<sup>8</sup>:

$$V_{\Lambda^*\Lambda^*}(r) = g_{\omega\Lambda^*}^2 \left(1 - \frac{1}{2} \frac{m_\omega^2}{M_{\Lambda^*}^2}\right) Y_\omega(r) - g_{\sigma\Lambda^*}^2 \left(1 - \frac{1}{4} \frac{m_\sigma^2}{M_{\Lambda^*}^2}\right) Y_\sigma(r) + g_{\omega\Lambda^*}^2 \frac{1}{6} \left(\frac{m_\omega}{M_{\Lambda^*}}\right) Y_\omega(r) (\vec{\sigma}_1 \cdot \vec{\sigma}_2), \quad (2)$$

where  $M_{\Lambda^*} = 1405$  MeV,  $m_i$  are the meson masses,  $g_{i\Lambda^*} = \alpha_i g_{iN}$  are the corresponding coupling constants with  $g_{iN}$  taken from the HS model<sup>9</sup>, and  $Y_{i=\sigma,\omega}(r) = \exp(-m_i r)/(4\pi r)$ . In the above expressions, the mass correction factors ( $\sim m_i/M_{\Lambda^*}$  and  $m_i^2/M_{\Lambda^*}^2$ ) as well as the spin-spin interaction terms ( $\sim (\vec{\sigma}_1 \cdot \vec{\sigma}_2)$ ) are included.

In the calculations we fit either the value of  $\alpha_\sigma$  and kept  $\alpha_\omega$  fixed to 1 or vice versa in order to get the binding energy of the  $\Lambda^*\Lambda^*$  system  $B_{\Lambda^*\Lambda^*} = 40$  MeV. We present here only selected results for  $\alpha_\sigma \neq 1$ .

In Fig. 1, left panel, we show the binding energy per  $\Lambda^*$ ,  $B/A$ , as a function of mass number in few-body  $\Lambda^*$  nuclei, calculated within the SVM approach for the Machleidt potential (1). When the spin-spin interaction is omitted, the binding energy per particle is rapidly increasing with  $A$ , reaching  $B/A \approx 130$  MeV for  $A=6$ . The mass corrections have almost no effect on the calculated values of  $B/A$ . On the other hand, when the spin-spin interaction is taken into account, the increase of  $B/A$  is considerably less steep. The corresponding rms radius of the considered  $\Lambda^*$  nuclei is presented in the right panel. The rms radius is extremely small, hardly exceeding the value 0.8 fm even if the spin-spin interaction is included.

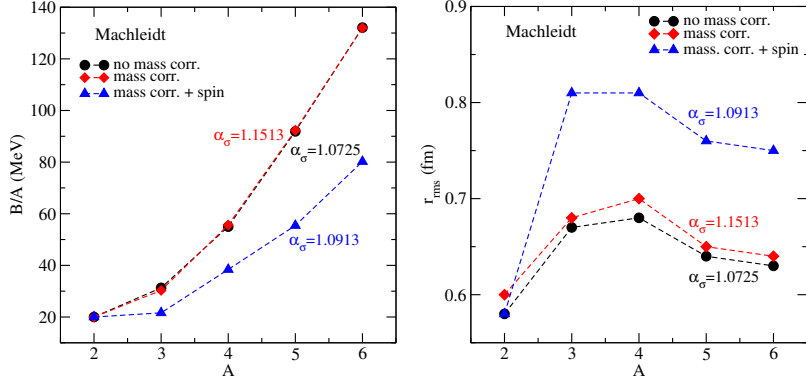


Fig. 1. Binding energy of  $\Lambda^*$  nuclei per particle,  $B/A$  (left panel) and rms radius (right panel) of few-body  $\Lambda^*$  systems as a function of mass number  $A$ , calculated using the Machleidt potential with and without mass corrections, as well as including spin-spin interaction.

### 3. $\Lambda^*$ Many-Body Systems

As the next step, we explored many-body systems composed solely of  $\Lambda^*$  hyperons within the RMF framework<sup>5</sup>, where the interaction among  $\Lambda^*$ 's is mediated by the exchange of the scalar  $\sigma$  and vector  $\omega$  meson fields. The underlying Lagrangian density is of the form

$$\mathcal{L} = \bar{\Lambda}^* [i\gamma^\mu D_\mu - (M_{\Lambda^*} - g_{\sigma\Lambda^*}\sigma)]\Lambda^* + (\sigma, \omega_\mu \text{ free-field terms}), \quad (3)$$

where  $D_\mu = \partial_\mu + ig_{\omega\Lambda^*}\omega_\mu$ . It is to be noted that the isovector-vector  $\vec{\rho}$  and Coulomb fields were not taken into account since the  $\Lambda^*$  is a neutral  $I = 0$  baryon. First calculations were performed using the linear HS model<sup>9</sup> with the coupling constants scaled by  $\alpha_1$ ,  $g_{i\Lambda^*} = \alpha_i g_{iN}$ , determined by fitting  $B_{\Lambda^*\Lambda^*}$  (see previous section). For comparison, we performed also calculations using the nonlinear NL-SH model<sup>10</sup>. The corresponding scaling parameter  $\alpha_\sigma$  was fitted to yield the binding energy of the  $8\Lambda^*$  system calculated within the HS model. We explored  $\Lambda^*$  nuclei with closed shells and solved self-consistently the coupled system of the Klein-Gordon equations for meson fields and the Dirac equation for  $\Lambda^*$ .

The results of our RMF calculations are summarized in Fig. 2. In the left panel, the binding energy per particle,  $B/A$ , is plotted as a function of mass number  $A$ , calculated within the RMF HS model with the properly rescaled  $\sigma$  meson coupling constant corresponding to the  $\Lambda^*$  potentials (1) and (2). For comparison,  $B/A$  calculated within the RMF NL-SH model in

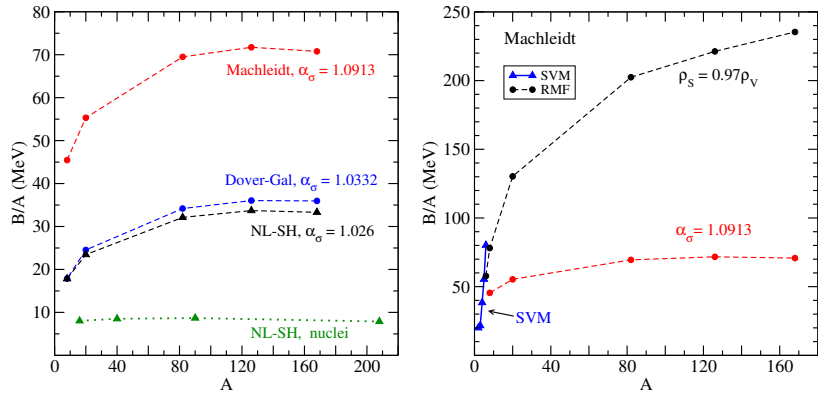


Fig. 2. Left panel: Binding energy of  $\Lambda^*$  nuclei per particle,  $B/A$  as a function of mass number  $A$ , calculated within the HS and NL-SH models;  $B/A$  in atomic nuclei ('nuclei') is shown for comparison. Right panel: Comparison of  $B/A$  calculated in  $\Lambda^*$  nuclei within the HS model for the Machleidt potential (red line) with a similar calculation using  $\rho_s = 0.97\rho_v$  (black line);  $B/A$  in few body systems, calculated within the SVM is shown for comparison. See text for details.

$\Lambda^*$  nuclei as well as in ordinary nuclei is shown as well. The binding energy per  $\Lambda^*$  saturates with the number of constituents for  $A \geq 120$  in all versions considered and reaches tens of MeV depending on the potential used. Calculations with the rescaled  $\omega$  coupling constant yield similar saturation curves for  $B/A$  in  $\Lambda^*$  nuclei.

The observed saturation originates from the Lorentz covariance which introduces two types of baryon densities — the scalar density  $\rho_s$  associated with the attractive  $\sigma$  field and the vector (baryon) density  $\rho_v$  associated with the repulsive  $\omega$  field. In dense matter, the scalar density decreases with respect to the vector density since  $\rho_s \sim M^*/E^* \rho_v$  where  $\frac{M^*}{E^*} < 1$ , and  $M^* = M - g_{\sigma B} \langle \sigma \rangle$  is baryon effective mass. As a consequence, the attraction from the scalar field is reduced considerably at higher densities. This is illustrated in Fig. 2 (right panel), where we present the RMF calculation of  $B/A$  in  $\Lambda^*$  nuclei, in which we replaced the scalar density  $\rho_s$  by a density equal to  $0.97\rho_v$  (this corresponds to  $\rho_s/\rho_v$  in  $^{16}\text{O}$ ). The binding energy per  $\Lambda^*$  (denoted ' $\rho_s = 0.97\rho_v$ ') is rapidly increasing in this case, similar to the SVM calculations (also shown for comparison), and does not seem to saturate within the explored mass range, unlike  $B/A$  evaluated using the 'dynamical' scalar density  $\rho_s$  (denoted ' $\alpha_\sigma = 1.0913$ '). It is to be noted that the central density of calculated  $\Lambda^*$  nuclei saturates as a

function of  $A$  as well, reaching about twice nuclear matter density.

Finally, we introduced the  $\Lambda^*$  absorption and explored how the  $\Lambda^*$  decay width changes in the medium. We considered the two-body decay  $\Lambda^* \Lambda^* \rightarrow \Lambda \Lambda$  in the  $1s$  state, described by the imaginary part of an optical potential in a ' $t\rho$ ' form with the amplitude fitted to assumed width  $\Gamma_{\Lambda^* \Lambda^*} = 100$  MeV at threshold, taking into account phase space suppression. We found that the conversion widths, despite being suppressed to some extent in the  $\Lambda^*$  nuclei (by 28% in  $A=8$  systems and by less than 1% in  $A=168$  systems), remain considerable and the  $\Lambda^* \Lambda^*$  pairs will thus inevitably decay.

#### 4. Summary

We performed calculations of  $\Lambda^*$  nuclei with various  $\Lambda^*$  interaction strengths compatible with the value  $B_{\Lambda^* \Lambda^*} = 40$  MeV of the YA model<sup>1</sup> in order to demonstrate that the  $\Lambda^*$  stable-matter scenario<sup>3</sup> is not supported by standard many-body approaches. We found that the binding energy per  $\Lambda^*$  in many-body systems saturates in all cases for  $A \geq 120$  at values far below  $\approx 290$  MeV, which is the energy required to reduce the  $\Lambda(1405)$  mass in the medium below the mass of the lightest hyperon  $\Lambda(1116)$ . The  $\Lambda^*$  matter is thus highly unstable against strong interaction decay.

#### Acknowledgment

This work was partly supported by the Czech Science Foundation GACR grant 19-19640S.

#### References

1. T. Yamazaki and Y. Akaishi, Phys. Rev. **C 76**, 045201 (2007).
2. J. Hrtánková, N. Barnea, E. Friedman, A. Gal, J. Mareš and M. Schäfer, Phys. Lett. **B 785**, 90 (2018).
3. Y. Akaishi and T. Yamazaki, Phys. Lett. **B 774**, 552 (2017).
4. K. Varga and Y. Suzuki, *Stochastic Variational Approach to Quantum-Mechanical Few-Body Problems* (Springer 1998).
5. B. D. Serot and J. D. Walecka, Adv. Nucl. Phys. **16**, 1 (1986).
6. E. Friedman and A. Gal, Nucl. Phys. **A 959**, 66 (2017).
7. C. B. Dover and A. Gal, Prog. Part. Nucl. Phys. **12**, 171 (1984).
8. R. Machleidt, Adv. Nucl. Phys. **19**, 189 (1989).
9. C. J. Horowitz and B. D. Serot, Nucl. Phys. **A 368**, 503 (1981).
10. M. M. Sharma, M. A. Nagarajan, P. Ring, Phys. Lett. **B 312** (1993) 377.